

Multi-channel respiratory signal detection system for 4D-CT in radiotherapy by measuring the back pressure

Yuan Zheng, Yahui Peng, Haizhen Yue, Haiyan Xiang and Yi Du

Abstract— This study proposes a novel respiratory signal detection system for 4D-CT in radiotherapy by measuring back pressure changes at multiple positions on CT couch. The 12-channel pressure sensor is fixed on CT couch to obtain patient's back pressure signal. The 12-channel signal is transmitted to a PC at a sampling rate of 50 Hz after a signal conditioning circuit and an analog-digital converter. The amplitude of pressure changes is characterized to select the optimal channel. This system is validated by comparing with the respiratory signal collected synchronously with a real-time position management (RPM) system on 10 healthy volunteers. The correlation coefficient between the signals is 0.82 ± 0.09 (standard deviation) and the time shift is 0.32 ± 0.15 second. We conclude that the back pressure signal acquired by the proposed system has the potential to replace the clinical RPM system for respiratory signal detection in 4D-CT data acquisition.

I. INTRODUCTION

Respiratory motion management is a crucial issue in clinical radiotherapy especially in lung, liver and pancreas tumor treatments [1]. For patients with these tumor sites, 4D-CT is routinely prescribed to effectively evaluate the respiratory motion in tumor targets [2]. Compared with conventional CT, 4D-CT is to deliver series of three-dimensional anatomical images that are correlated with temporal phases.

During 4D-CT, the patient respiratory signal is measured and directed to the CT scanner to guide the process of data acquisition [4]. The prevailing respiratory signal detection methods in current radiotherapy clinic fall into four categories: (1) airflow measurement system, such as the active respiration control (ABC) system by Elekta AB [5]; (2) external marker based systems, such as the real-time positioning management (RPM) system by Varian [6]; (3) body surface expansion monitoring system, such as the AZ-733V belt by Anzai Medical [7]; (4) body surface undulation monitoring product such as the Sentinel by C-RAD. The respiratory movement of the human body is completed by the coordinated movement of multiple muscle groups. Actually, respiration is a complex physiological activity involved with multiple muscle groups. For patients lying on the CT couch in supine, the back muscles related to respiration (such as latissimus dorsi and erector

spinae) contract and relax regularly with the respiratory movement, and thus the pressure between the back and the couch surface changes simultaneously. Inspired by this, this paper aims to develop a novel respiratory signal detection method via measuring pressure changes on the body back [8]. Since different positions on the back have different sensitivity to respiratory movement [9], 12 pressure sensors are fixed on the CT couch to collect pressure signals at different positions on the back, and the signal of the channels most affected by respiration is filtered through signal-to-noise ratio. Then the respiratory signal is extracted from raw pressure signal by the method of empirical mode decomposition [10]. As validation, the RPM system is used as benchmark to compare the correlation and time shift with the proposed system.

II. SYSTEM DESCRIPTION

The system introduced in this paper includes the following three parts: (1) 12-channel pressure sensor; (2) signal processing module; (3) a personal computer including software for real-time display of pressure signal and related signal processing algorithms.

A. 12-channel Pressure Sensor

The pressure sensor used in this system is based on the principle of piezoresistive effect to achieve pressure detection. We have noticed that for different patients, the pressure at different positions on the back has different sensitivity to respiration in clinical tests. The pressure at some positions changes significantly with respiration, while some are minimally affected by respiration. Therefore, the position of the pressure sensor needs to be adjusted depending on experience of the physicist to detect qualified signals, which is not conducive to clinical applications. Multi-channel pressure sensor is used to solve this problem. The 12-channel pressure sensor is fixed on the CT couch, as shown in Figure 1, and simultaneously detects the pressure of multiple positions that may be affected by respiratory movement.

*This work was supported in part by the Beijing Natural Science Foundation (1212011, 1202009), National Natural Science Foundation of China (12005007), National Key Research and Development Project (2019YFF01014405), Capital's Funds for Health Improvement and Research (2018-4-1027), Ministry of Education Science and Technology Development Center (2018A01019), Beijing Municipal Administration of Hospitals Incubating Program (PX2019042), Science Foundation of Peking University Cancer Hospital (2021-14, 2021-1). (Corresponding: Yahui Peng, yhpeng@bjtu.edu.cn; Yi Du, yi.du@hotmail.com)

Yuan Zheng and Yahui Peng are with the the School of Electronic and Information Engineering, Beijing Jiaotong University, 3 Shangyuancun, Beijing 100044, China.

Haizhen Yue, Haiyan Xiang and Yi Du are with the Key Laboratory of Carcinogenesis and Translational Research (Ministry of Education/Beijing), Department of Radiation Oncology, Peking University Cancer Hospital & Institute, 52 Fucheng Road, Beijing 100142, China.



Figure 1. 12-channel pressure sensor fixed on the CT couch.

B. Signal Processing Module

As shown in Figure 2, the signal processing module includes a signal conditioning circuit and a micro control board. Filtering circuit and amplifying circuit are used for preliminary processing of the raw signal to increase the signal-to-noise ratio. Arduino mega 2560 is a micro control board that provides a 10-bit analog-to-digital converter and transmits the converted digital signal to the personal computer through the USB interface.

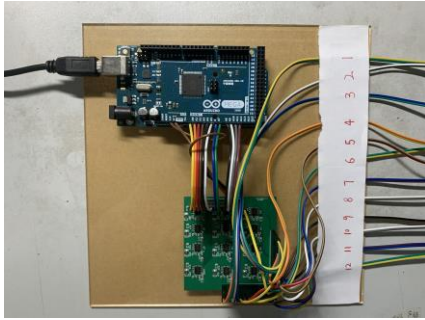


Figure 2. Signal processing module including a signal conditioning circuit, a control board and a USB interface.

C. Channel Selection Method

The extracted channel signal should have obvious respiratory waveforms and less noise. The algorithm of channel selecting is as follows.

- (1) Calculate the power of the component whose frequency is 0.1-0.3Hz, which can represent the power of the respiratory signal;
- (2) Calculate the power of the component whose frequency is above 0.3Hz, which can represent the power of high-frequency noise in the raw signal;
- (3) Calculate the signal-to-noise ratio;
- (4) The pressure signal of the channel with the largest signal-to-noise ratio is the screening result.

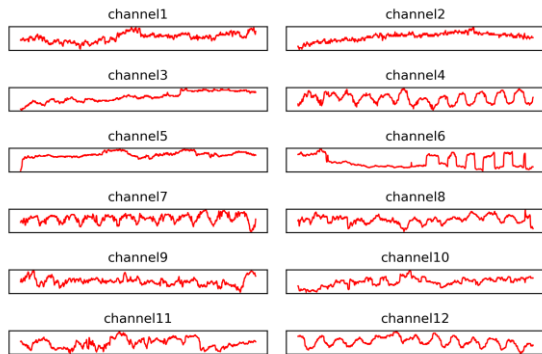


Figure 3. 12-channel pressure signal obtained on the back of a volunteer.

As shown in Figure 3, the pressure signals of the 12 channels are significantly different. The calculation result of the signal-to-noise ratio defined by the above method for this volunteer is shown in Table 1. The result shows that the data of the 12th channel has the highest signal-to-noise ratio, followed by the 4th channel. This result is consistent with the waveform in Figure 3.

TABLE I. THE SIGNAL-TO-NOISE RATIO OF THE ABOVE VOLUNTEER'S DIFFERENT CHANNEL DATA

Channel index	SNR / dB
1	2.75
2	-1.28
3	6.91
4	12.43
5	8.07
6	7.56
7	7.94
8	7.09
9	5.92
10	5.02
11	5.68
12	13.40

D. Respiratory signal extraction method

The empirical mode decomposition (EMD) is applied to separate the respiratory signal from the pressure signal. EMD is an adaptive signal time-frequency analysis method, which is suitable for the decomposition of stationary and non-stationary signals. EMD decomposes the signal into a series of intrinsic mode function (IMF), and each IMF represents an oscillation mode [11]. The respiratory signal is reconstructed by superimposing the IMFs that conform to the respiratory signal mode. As shown in Figure 4, the raw data can be decomposed into ten imfs and a residual, where imf6 conforms to the characteristics of the respiratory signal.

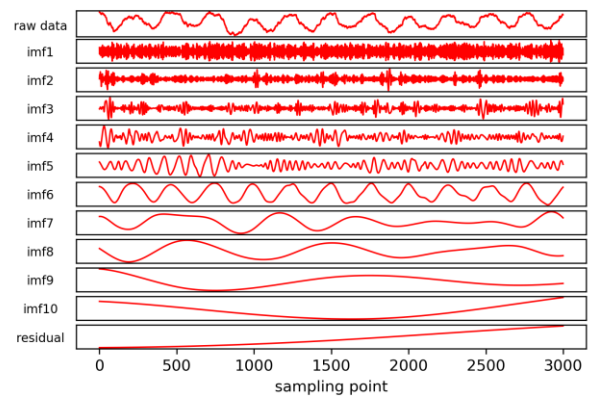


Figure 4. Result of EMD of the pressure signal of a volunteer.

E. Peaks and Valleys Detection and Phase Calculation

The extreme points of the discrete time signal are defined as follows. The point where the amplitude at a certain time is greater than the amplitude of the adjacent time is the maximum

point. And the point where the amplitude at a certain time is less than the adjacent amplitude is the minimum point. The conventional extreme point definition method can search for the peaks and valleys of most respiratory signals, but for some respiratory signals with false peaks or valleys, misjudgment will be caused. The prominence defined in [12] can filter the extreme points obtained by the search. “True” respiratory signal peaks and valleys have greater prominence than “false” peaks and valleys, and the two can be distinguished when the prominence threshold is set to 0.01.

To determine the phase information, it is necessary to define the phase of three key moments in a respiratory cycle: expiration critical point-inhalation critical point-breathing critical point. We set 0, π , and 2π to be the phases of these three moments respectively. At any moment within these three moments, the calculation is performed according to the linear relationship. The peaks and valleys detection results and the phase calculation results are shown in Figure 5.

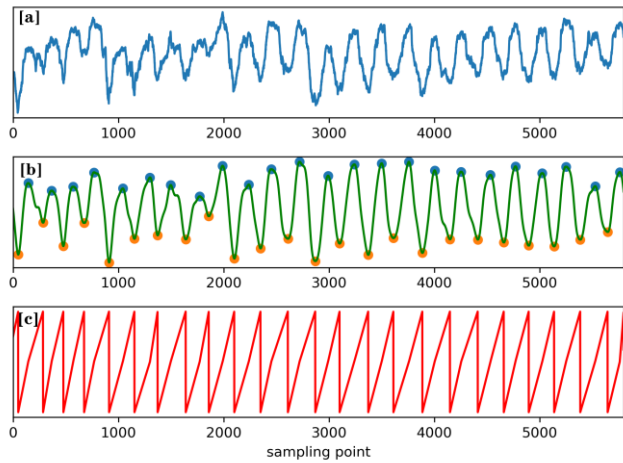


Figure 5. Result of peaks and valleys detection and phase calculation of a volunteer. (a) Raw signal. (b)Peaks and valleys detection. (c) Phase angle calculation.

III. SIGNAL ACQUISITION AND ANALYSIS

A. Signal Acquisition with RPM

The process of multi-channel pressure signal detection system and RPM system for signal collection is as follows.

- (1) 12 pressure sensors are symmetrically fixed on the CT couch;
- (2) The volunteer lies on the CT couch and ensures that the back of body is effectively attached to the 12 sensors;
- (3) Fix the marker box of the RPM system on the surface of the volunteer’s abdomen, and ensure that the regular fluctuations of the marker are captured in the camera;
- (4) When the volunteer’s breathing is subtle, turn on the recording of these two systems at the same time;
- (5) Ensure that the volunteer’s recorded signal length exceeds 1 minute, and then turn off the two systems.

The signal acquisition scene is as shown in Figure 6. The respiratory signals of 10 test subjects are collected simultaneously by the system of this paper and the RPM system.



Figure 6. Synchronous signal acquisition of pressure acquisition system and RPM system.

B. Signal Analysis

Correlation analysis is used to evaluate the similarity of the amplitude information of the pressure signal and the RPM signal, and time-shift analysis is used to evaluate the similarity of the phase information of the two. We uniformly intercept all sample data for 1 minute for analysis.

The Pearson’s correlation coefficient is computed between the RPM signal and pressure signal as described in (1). Here s_{rpms} and s_{ps} are the amplitudes of RPM and pressure signals respectively and σ is the standard deviation.

$$PCC = \frac{\sum_{i=1}^n (s_{rpms}(i) - \bar{s}_{rpms})(s_{ps}(i) - \bar{s}_{ps})}{(n-1)\sigma_{rpms}\sigma_{ps}} \quad (1)$$

The time shift is defined by calculating the time difference between the RPM signal and the pressure signal at all critical points of respiration within a specified time length. The time shift is computed as described in (2). Here t_{rpms} and t_{ps} are the interval between the peaks and the valleys of the respiratory signal, and k is the total number of peaks and valleys in 1 minute.

$$tS = \frac{\sum_{j=1}^k |t_{rpms}(j) - t_{ps}(j)|}{k} \quad (2)$$

IV. RESULTS

Figure 7 shows the comparison result of a volunteer’s pressure signal and RPM signal amplitude and phase angle. The indicators for comparison include the correlation coefficient and time shift of the two signals.

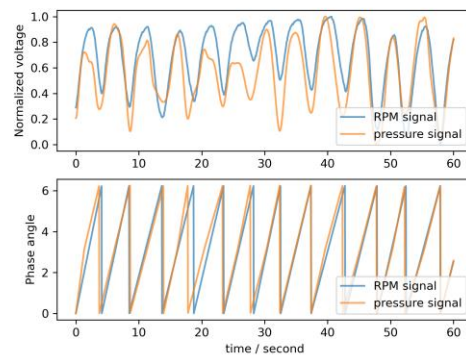


Figure 7. Comparison of RPM signal and pressure signal of a volunteer.

A. Correlation of Signals

As shown in Table 2, across all the 10 volunteers, the largest correlation coefficient reaches 0.91, and the smallest correlation coefficient is 0.65 when the back-pressure signal is greatly affected by body movement. The average value of the correlation coefficient of the 10 volunteers reaches 0.82 ± 0.09 (1SD).

TABLE II. CORRELATION OF SIGNALS

Patient ID	Correlation coefficient
1	0.84
2	0.88
3	0.85
4	0.65
5	0.68
6	0.90
7	0.83
8	0.91
9	0.88
10	0.77

B. Time Shift of Signals

As shown in Table 3, the smallest time shift between RPM signal and pressure signal reaches 0.13 second and the largest time shift reaches 0.62 second. The average value of the time shift of the 10 volunteers reaches 0.32 ± 0.15 (1SD).

TABLE III. TIME SHIFT OF SIGNALS

Patient ID	Time shift / second
1	0.26
2	0.39
3	0.17
4	0.31
5	0.43
6	0.13
7	0.27
8	0.13
9	0.41
10	0.62

V. CONCLUSION AND FUTURE WORKS

The signals detected by the proposed respiratory signal acquisition system are highly correlated with the RPM signals, and the application of multi-channel sensor and channel selection algorithms decrease the uncertainty of the back respiratory measurement position and optimized the signal quality. As proof-of-concept, there are some limitations in this study. First, we found that the respiratory phases of the upper back and the lower back are not the same, which may obscure the respiratory phase calculation. Therefore, it is necessary to analyze the back respiratory phase information of more patients in order to find the laws

that fit different groups of people. Second, the volunteer cohort is not large enough to draw definitive conclusions on channel selection, which may be affected by gender, age, body type et al.

REFERENCES

- [1] J. R. McClelland, D. J. Hawkes, T. Schaeffter, and A. P. King, "Respiratory motion models: A review," *Med. Imag. Anal.*, vol. 17, no. 1, pp. 19-42, 2013.
- [2] S. B. Jiang, "Technical aspects of image-guided respiration-gated radiation therapy," *Med Dosim*, vol. 31, no. 2, pp. 141-151, 2006.
- [3] C. Cavedon, "Real-time control of respiratory motion: Beyond radiation therapy," *Phys Med*, vol. 66, pp. 104-112, 2019.
- [4] W. Lu, K. J. Ruchala, M. L. Chen, Q. Chen, and G. H. Olivera, "Real-time respiration monitoring using the radiotherapy treatment beam and four-dimensional computed tomography (4DCT)--a conceptual study," *Phys Med Biol*, vol. 51, no. 18, pp. 4469-4495, 2006.
- [5] M.-C. Jeon, M.-S. Han, H.-S. Lim, J.-U. Jang, S.-J. Yoo, S.-Y. Seo, and C.-G. Kim, "The analysis of doses and image at chest radiography using an Active Breathing Coordinator (ABC) system," *Cluster Computing*, vol. 18, no. 2, pp. 659-665, 2015.
- [6] S. A. Nehmeh, Y. E. Erdi, T. Pan, E. Yorke, G. S. Mageras, K. E. Rosenzweig, H. Schoder, H. Mostafavi, O. Squire, A. Pevsner, S. M. Larson, and J. L. Humm, "Quantitation of respiratory motion during 4D-PET/CT acquisition," *Med Phys*, vol. 31, no. 6, pp. 1333-1338, 2004.
- [7] X. A. Li, C. Stepaniak, and E. Gore, "Technical and dosimetric aspects of respiratory gating using a pressure-sensor motion monitoring system," *Med Phys*, vol. 33, no. 1, pp. 145-154, 2006.
- [8] L. Rosales, Bo Y. Su, M. Skubic, and K. C. Ho, "Heart rate monitoring using hydraulic bed sensor ballistocardiogram1," *Journal of Ambient Intelligence and Smart Environments*, vol. 9, no. 2, pp. 193-207, 2017.
- [9] X. Zhang, J. Tang, G. C. Sharp, L. Xiao, S. Xu, and H. M. Lu, "A new respiratory monitor system for four-dimensional computed tomography by measuring the pressure change on the back of body," *Br J Radiol*, vol. 93, no. 1108, pp. 20190303, 2020.
- [10] D. Labate, F. L. Foresta, G. Occhiuto, F. C. Morabito, A. Lay-Ekuakille, and P. Vergallo, "Empirical Mode Decomposition vs. Wavelet Decomposition for the extraction of respiratory signal from single-channel ECG: A comparison," *IEEE Sensors Journal*, vol. 13, no. 7, pp. 2666-2674, 2013.
- [11] W. Karlen, A. Garde, D. Myers, C. Scheffer, J. M. Ansermino and G. A. Dumont, "Estimation of respiratory rate from photoplethysmographic imaging videos compared to pulse oximetry," in *IEEE Journal of Biomedical and Health Informatics*, vol. 19, no. 4, pp. 1331-1338, 2015.
- [12] A. Kirmse, J. D. Ferranti, "Calculating the prominence and isolation of every mountain in the world," *Progress in Physical Geography*, vol. 41, no. 6, pp. 788-802, 2017.